

# A GMR Needle Probe to Estimate Magnetic Fluid Weight Density Inside Large Tumors

C.P. Gooneratne<sup>1</sup>, A. Kurnicki<sup>2</sup>, M. Iwahara<sup>1</sup>, M. Kakikawa<sup>1</sup>,  
S.C. Mukhopadhyay<sup>3</sup>, and S. Yamada<sup>1</sup>

<sup>1</sup> Kanazawa University, Kanazawa, Japan

<sup>2</sup> Lublin University of Technology, Lublin, Poland

<sup>3</sup> Massey University, Palmerston North, New Zealand

**Abstract.** In this paper we are proposing a needle-type GMR sensor to estimate magnetic fluid weight density inside large tumors. The application is hyperthermia therapy, a form of cancer treatment. Hyperthermia therapy utilizes the magnetic losses due to magnetization of magnetic nanoparticles by external alternating current magnetic fields. These magnetic losses can be dissipated in the form of heat depending on the thermal conductivity and heat capacity of the surrounding medium. The overall effect is an increase in temperature of the surrounding. This principle is applied to heat and destroy tumors since they are more sensitive to heat than normal healthy cells. Generally all parameters except the magnetic fluid weight density are known in the specific heat equation which governs the heat given in hyperthermia therapy to destroy cancer cells. Hence, accurate estimation of magnetic fluid weight density is critical for successful treatment. This paper presents a methodology to estimate magnetic fluid weight density inside the body and experimental results, by a needle-type GMR sensor.

## 1 Introduction

Magnetic fluids are colloidal mixtures consisting of superparamagnetic nanoparticles suspended in a carrier fluid, usually an organic solvent or water. Magnetite ( $\text{Fe}_3\text{O}_4$ ) is the most widely used and promising magnetic nanoparticle available today. Since magnetic fluids are stable, colloidal suspensions they possess a unique combination of fluidity and ability to interact and be influenced by magnetic fields. Superparamagnetic nanoparticles have controllable sizes ranging from a few nanometers, which places them at dimensions that are smaller than or comparable to those of a cell (10 – 100  $\mu\text{m}$ ), a virus (20 – 450 nm), a protein (5 – 50 nm) or a gene (2 nm wide and 10 – 100 nm long) [1]. Superparamagnetic nanoparticles are non-toxic and biocompatible which means that they are physiologically well tolerated. For example dextran magnetite has no measurable toxicity index  $\text{LD}_{50}$  [2]. There are many biomedical applications of magnetic fluid due to its special physical properties. Magnetic fluid is used as contrast agents in MRI and coupled with biological molecules and used in cell labeling and separation [3]. Superparamagnetic nanoparticles can also be controlled by an external magnetic field gradient so they are coupled with anti-cancer drugs in targeted drug delivery [4]. Furthermore they

resonantly respond to ac magnetic fields, which lead to a transfer of energy from the exciting field to the nanoparticle. This is exploited in hyperthermia therapy where the self heating properties of superparamagnetic nanoparticles can be used to deliver toxic amounts of heat to a tumor [5,6].

Cancer stages are usually categorized according to the size of the tumor and how much it has spread to other tissues and organs [7]. In later stage cancer (stages 3 and 4) the diameter of tumors is 50 mm or more (assuming tumors are spherical shaped). Hyperthermia therapy utilizes heat to destroy tumor cells. Magnetic nanoparticles can be used as self heating agents [8]. Magnetic fluid injected near the affected area inside the body is more readily taken up and hence easily entered into tumor cells compared to healthy cells. Tumor cells are more sensitive to heat than healthy cells [9]. Tumor cells exposed to temperatures in excess of 42.5 °C for a prolonged period of time are destroyed due to apoptosis [9,10]. However, the weight density of the magnetic nanoparticles is an important parameter for giving heat in such a way that it does not affect other healthy cells. Furthermore, magnetic fluid weight density along with applied magnetic flux density amplitude and exciting frequency is directly proportional to the specific heat capacity [11]. Magnetic fluid once injected into the affected area spreads inside tissue effectively reducing its content density, providing an obstacle for successful hyperthermia therapy. This is more complicated in larger cavities since it is difficult to retain magnetic nanoparticles in a large area. By taking into account the difference in magnetic flux density inside a magnetic fluid filled tumor and outside, the fabricated needle-type GMR sensor is proposed to estimate the weight density of the magnetic nanoparticles before and after treatment inside large cavities.

This purpose of this paper is to introduce a uniquely designed novel needle-type GMR sensor for application inside the body in a minimally low-invasive way. A theoretical basis for estimating magnetic fluid weight density inside the body is developed by obtaining a relationship between relative permeability and the magnetic fluid weight density as well as a relationship between the difference of magnetic flux density inside and outside a magnetic fluid filled cavity and the magnetic fluid weight density. An experimental setup, including the needle-type GMR sensor, a Helmholtz tri-coil, and an experimental method in which agar is injected with magnetic fluid to simulate actual clinical process is reported.

## 2 Analytical Analysis

Magnetic nanoparticles are assumed to be spherical in shape and uniformly distributed in the fluid as shown in figure 1. The relative permeability of magnetic nanoparticles and liquid are assumed to be infinity and one respectively. However, the magnetic nanoparticles have a cluster structure so a spherical structure model is assumed as shown in figure 1. Since there is space between the magnetic nanoparticles the space factor of spherical magnetite is considered and an equation defining the relationship between the relative permeability and weight density is obtained [11], as shown below.

$$\mu^* = 1 + C_d D_w / h_s \gamma_f \quad (D_w \ll 1) \quad (2.1)$$

where  $C_d$  ; Coefficient (theoretically, 4)  
 $D_w$  ; Magnetic fluid weight density (mgFe/ml)  
 $h_s$  ; Space factor of spherical magnetite (0.523)  
 $\gamma_f$  ; Specific gravity of magnetite (4.58)

From equation (2.1) it can be seen that the relative permeability is proportional to the magnetic fluid weight density. It is worth to note there is no effect due to the shape or size of the cavity. To confirm equation (2.1) experimental analysis was carried out with the aid of a vibrating sample magnetometer (VSM) as shown in figure 2. When magnetic fluid samples of different weight densities are placed within a uniform magnetic field (provided by the electromagnets in the VSM) and made to undergo sinusoidal motion (mechanically vibrated by the vibration unit) there will be a change in magnetic flux. This induces a voltage in the pick up coils of the VSM, which is proportional to the magnetic moment of the sample. The comparison of the experimental and theoretical results is shown in figure 3. It can be seen that the relative permeability is proportional to the magnetic fluid weight density. The theoretical and experimental results are also in good agreement.

Figure 4 shows a uniform magnetic flux density applied to a spherical cavity filled with magnetic fluid. The magnetic flux lines converge at the magnetic fluid filled cavity. This gives rise to a difference between the applied magnetic flux density  $B_0$ , and the magnetic flux density inside  $B_1$ , the cavity. The magnetic flux density at the centre of the cavity can be expressed as shown in equation (2.2).

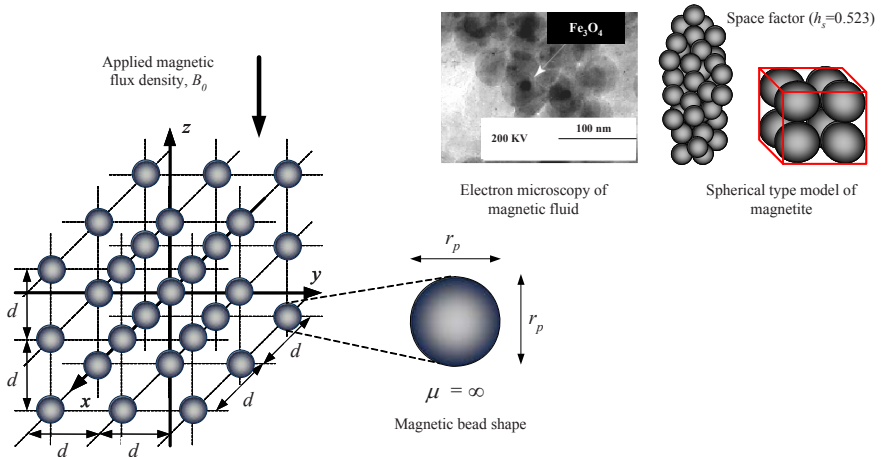


**Fig. 1.** Magnetic nanoparticle distribution

$$B_1 = \mu^* B_0 / \left\{ 1 + N(\mu^* - 1) \right\} \quad (\mu^* \approx 1) \quad (2.2)$$

where  $N$  is the demagnetizing factor of the cavity. Equation (2.1) is substituted into (2.2) to obtain the difference  $\delta$ , between the magnetic flux density inside and outside a magnetic fluid filled cavity.

$$\begin{aligned} \delta &= (B_1 - B_0) / B_0 \\ &\approx \left\{ C_d (1 - N) D_w / (h_s \gamma_f) \right\} \quad (D_w \ll 1) \quad (2.3) \end{aligned}$$

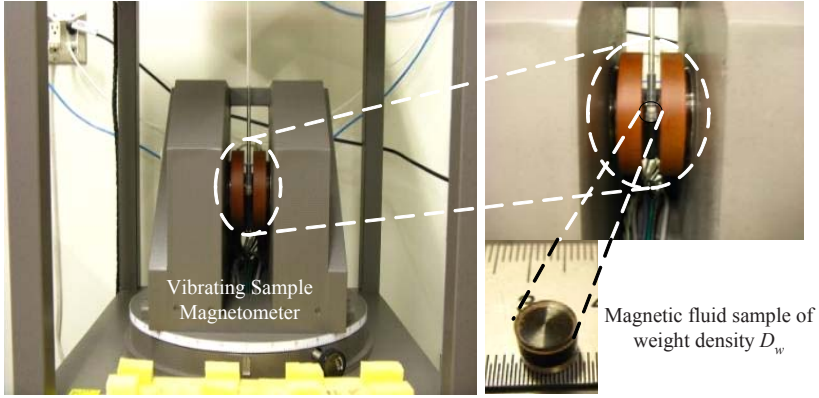


**Fig. 2.** Experimental setup – Vibrating sample magnetometer

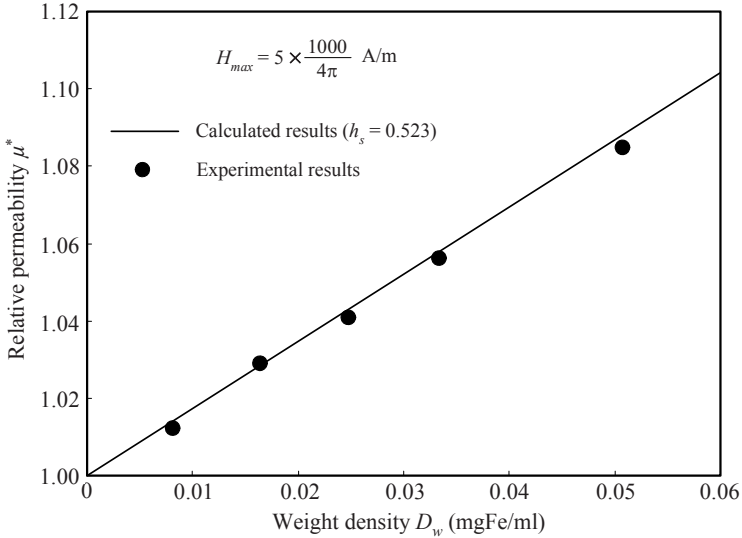


**Fig. 3.** Relationship between relative permeability and magnetic fluid weight density

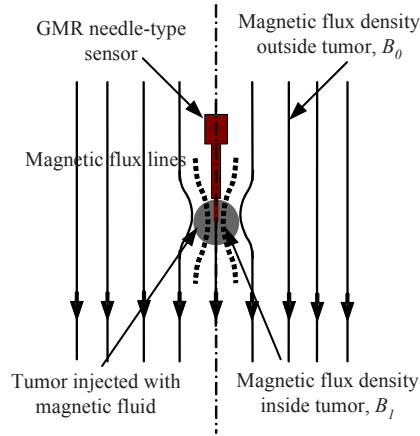


**Fig. 4.** Spherical magnetic fluid filled cavity under the influence of a uniform magnetic flux density

It can be seen from (2.3) that the magnetic fluid weight density can be calculated from the difference between the magnetic flux density inside and outside a magnetic fluid filled cavity. Magnetic fluid weight density is also proportional to the change ratio of magnetic flux density. The demagnetizing factor  $N$ , which depends on the shape and size of the cavity, influences the estimation of magnetic fluid weight density.

### 3 Needle-Type GMR Sensor

The fabricated needle-type GMR sensor as shown in figure 5 is the key feature of this research. The needle is made of a compound of Aluminium Oxide and Titanium Carbide ( $\text{Al}_2\text{O}_3/\text{TiC}$ ) and 20 mm in length (15 mm is available to be inserted inside the body). Referring to figure 5 it can be seen that the GMR sensors in the needle probe are designed as a bridge circuit. At the tip of the needle there is a sensing area of  $75 \times 40 \mu\text{m}$ . The three other GMR sensors of the bridge circuit are placed near the bonding pads.

Consider the event where the tip of the needle is inserted into the centre of a cavity (as explained in section 2 and figure 4), under a uniform magnetic flux density ( $B_0$ ). The four GMR sensors are exposed to  $B_0$ , assuming that the cavity is empty (permeability of 1 can be assumed inside and outside the cavity). So there is no change in magnetic flux density inside and outside the cavity since  $B_1$  is equal to  $B_0$ . However, when the cavity is filled with magnetic fluid the permeability inside is greater than outside the cavity. Hence, the GMR sensing area at the tip of the needle is exposed to a magnetic flux density  $B_1$ , which is higher than the applied magnetic flux density  $B_0$ . However, since the other three sensors are located further up near the bonding pads, and hence outside the magnetic fluid filled cavity, they will still be exposed to the applied magnetic flux density. This way the magnetic flux density inside a magnetic fluid filled cavity ( $B_1$ ) and outside the cavity ( $B_0$ ) can be measured simultaneously.

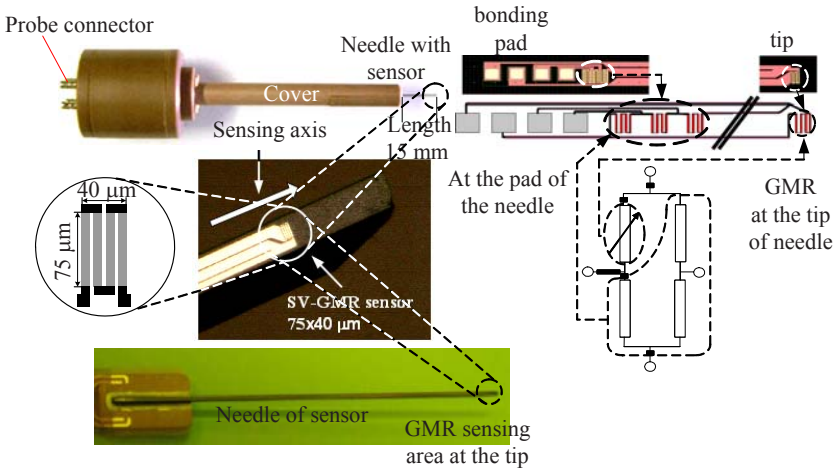


**Fig. 5.** Needle-type GMR sensor

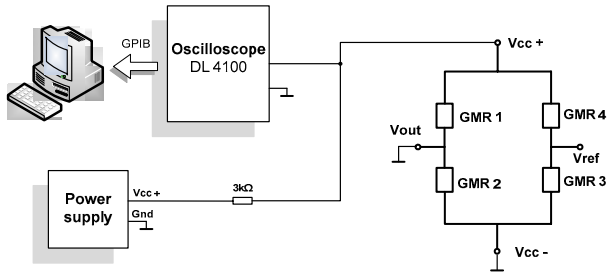


**Fig. 6.** Experimental setup for small signal ac characterization of needle-type GMR sensor

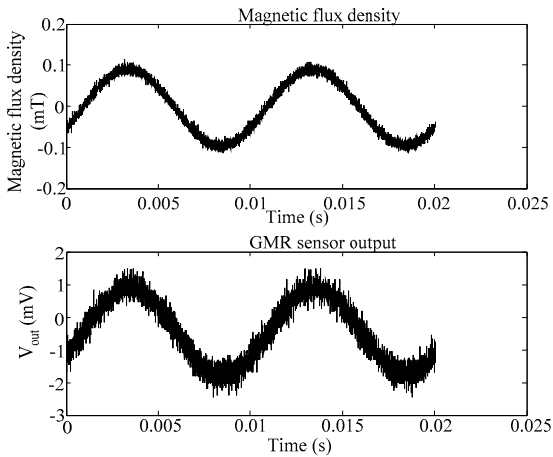


**Fig. 7.** GMR sensor output for an ac magnetic flux density of 0.1 mT

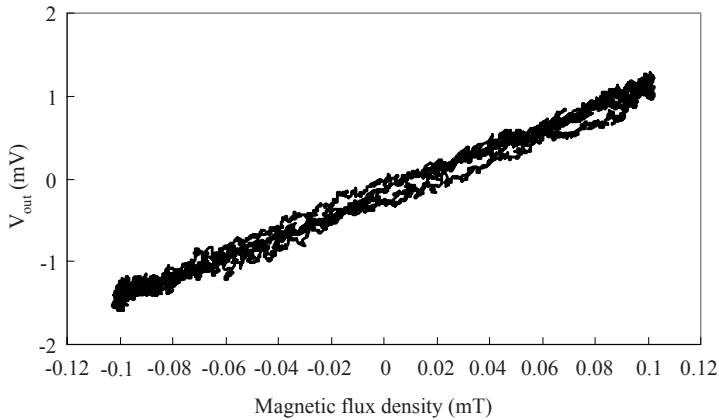


**Fig. 8.** Small signal ac characterization of GMR sensor at 100 Hz in the sensitive direction

The sensitivity of the needle-type GMR sensor in its sensitive axis was measured as shown in figure 6. The output from the GMR sensing area at the tip as was measured for an ac magnetic flux density of 0.1 mT as shown in figure 7. The results were analyzed by Yokogawa DL4100 oscilloscope and the data was transferred by general purpose interface bus (GPIB) to a personal computer for analysis. The small signal ac characteristics of the needle-type GMR sensor are shown in figure 8. It can be seen that the sensitivity is approximately 13 mV/mT.

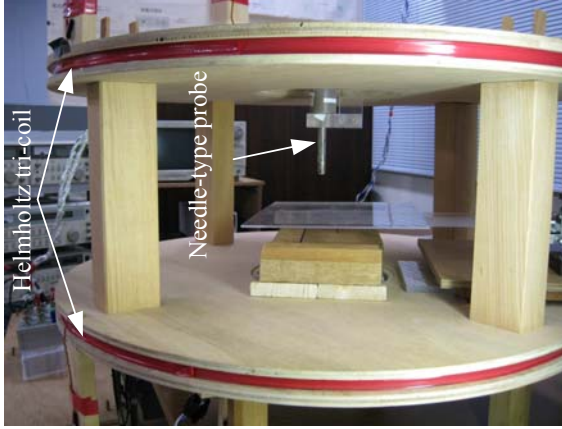
#### 4 Measurement Methodology

Since experiments are to be performed with low concentration magnetic fluid it is important that the applied magnetic flux density is at least  $1/10^{\text{th}}$  more uniform than the expected change in magnetic flux density inside and outside a magnetic fluid filled cavity. A Helmholtz tri-coil [12,13] as shown in figure 9 is fabricated to provide a uniform magnetic flux density. The Helmholtz tri-coil produces a uniform magnetic flux density of 0.1 mT at 100 Hz for experiments. The contour plot of error less than 0.01 % is shown in figure 10. The fluctuation of the magnetic flux density is 0.01 %, 0.03 m in the axial and radial direction from the midpoint.

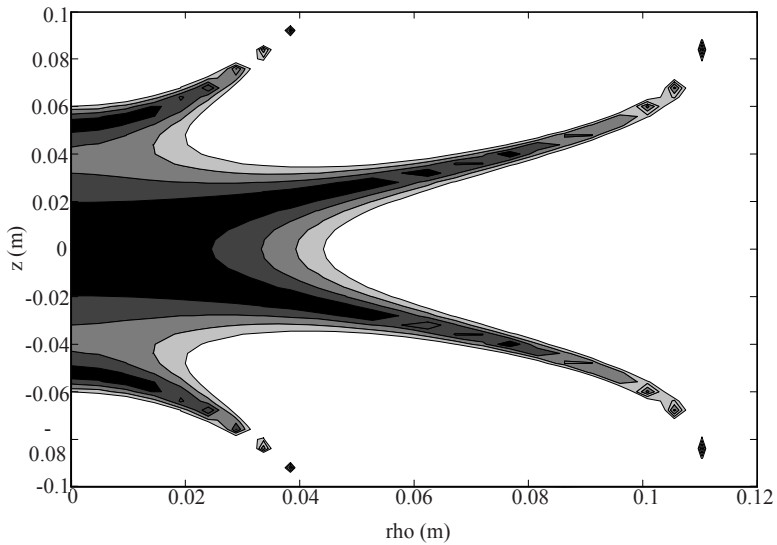
The experiment method for small cavities simulating  $1/2^{\text{nd}}$  stage cancerous tumors (less than 20 mm diameter) involves inserting the sensor needle at the centre of the cavity, where the magnetic flux density is most uniform. The experimental method for large cavities [13] is shown in figure 11. Since the sensor needle is only 15 mm in length it cannot be inserted to the centre of large cavities (larger than 30 mm in height). Also stage 3-4 cancerous tumors are generally more than 50 mm in diameter. The method proposed involves estimating the change in magnetic flux density at 20 mm steps (approximate distance between the sensing area at the tip and the three sensing areas near the bonding pads of the needle-type probe) as shown in

figure 11. The total change in the magnetic flux density is calculated by summing the change in magnetic flux densities at each step as shown below [13].

$$B_{TotalChange} = \sum_{i=0}^n (B_{i+1} - B_i) \quad (4.1)$$



**Fig. 9.** Helmholtz tri-coil



**Fig. 10.** Contour error plot (0.01 %) for Helmholtz tri-coil



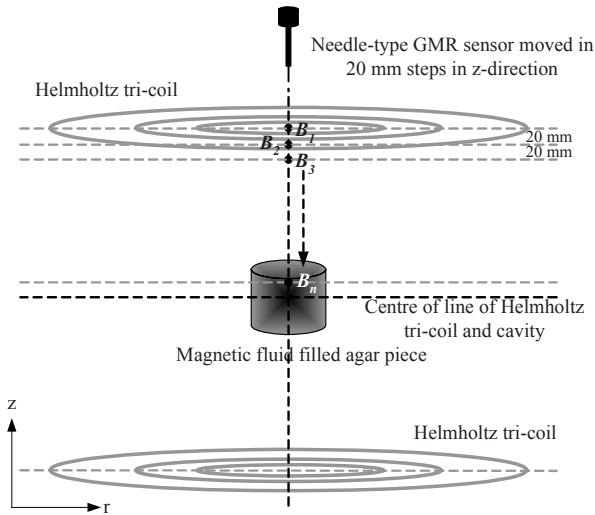


Fig. 11. Experimental method for large cavities

## 5 Experimental Results

The experimental setup is shown in figure 12. The Sony Tektronix AF5310 function generator provided the ac current at 100 Hz frequency. The function generator was connected to a NF Electronic Instrument 4055 high speed amplifier and the output was fed into the Helmholtz tri-coil. A current clamp probe connected to a Hioki 3272 power supply was connected to the Helmholtz tri-coil so that the current waveform could be analyzed using the Yokogawa DL4100 oscilloscope. The results from the bridge output of the sensor were analyzed through the NF electronics LI5640 lock-in amplifier.

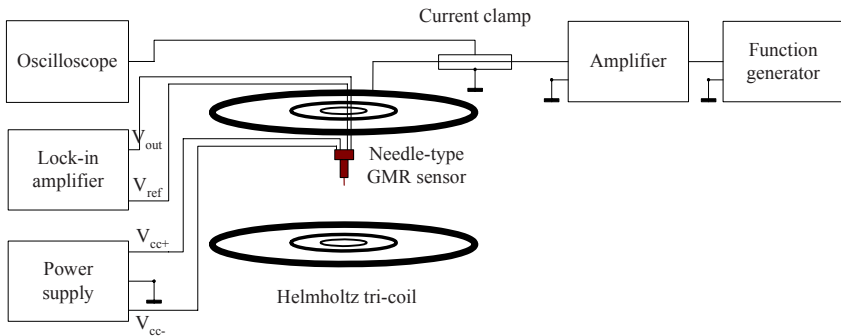
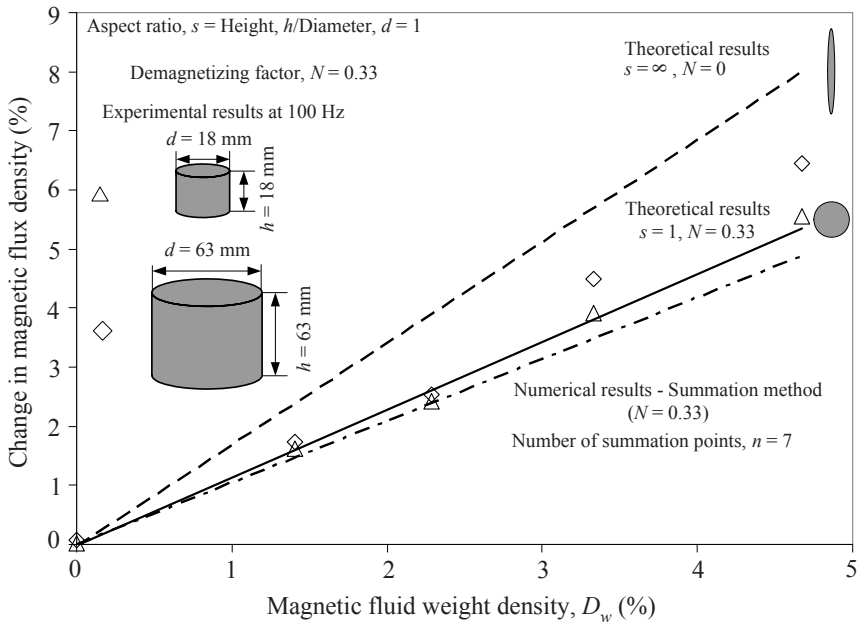


Fig. 12. Experimental setup

The demagnetizing factor  $N$ , of a cavity depends on the aspect ratio  $s$ . The aspect ratio of a cavity  $s = (\text{long axis}/\text{diameter})$ . Cylindrical agar cavities of diameter 18 and 63 mm ( $s = 1$ ) were injected with magnetic fluid. The needle-type sensor is then applied as explained in section 2 for 18 mm cavities and section 4 for 63 mm cavities. The experimental results are shown in figure 13. It can be seen that the total change in the magnetic flux density increases with weight density of the magnetic fluid. Moreover, the experimental results for large cavities compare favourably with theoretical results based on ellipsoidal cavities, numerical results obtained by numerical modelling and experimental results obtained for small cavities.

Figure 14 shows the results obtained for different size cylindrical agar cavities ( $s = 1$ ) for a weight density of 2.286 %. In previous experiments done on smaller cavities [14], equation (2.3) has been verified for a range of sizes. It was shown that the change in magnetic flux density did not vary so much between different size cavities as long as  $s$  and hence  $N$  remained the same. The change in magnetic flux density only increased with increasing magnetic fluid weight density. However, it must be noted that these experiments were performed with cavities smaller than 30 mm in diameter, hence allowing the insertion of the needle tip to the centre of the cavity. In the experiments performed in this paper the larger the cavity the further away it would be from the centre of the cavity (where the magnetic flux density is the greatest) as shown in table 1. Thus, as diameter and/or



**Fig. 13.** Estimation of magnetic fluid weight density inside large cavities by measuring the change in magnetic flux density by the needle-type GMR sensor

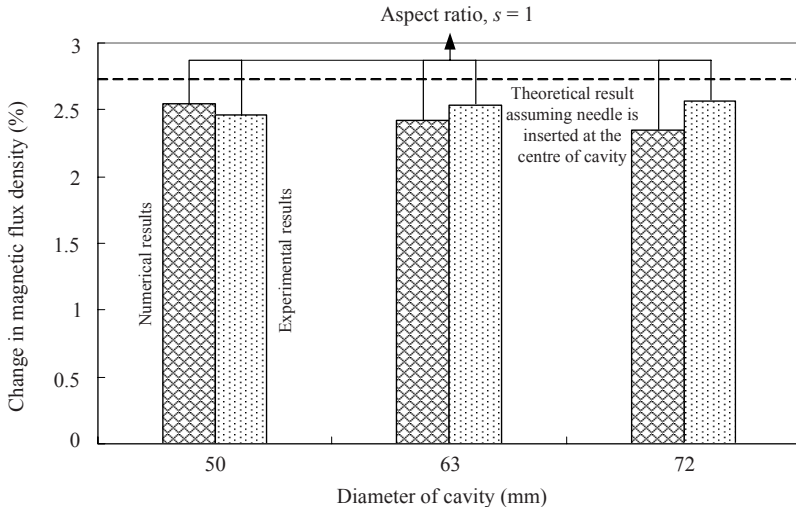


**Fig. 14.** Estimation of magnetic fluid weight density in different sized cavities for  $D_w = 2.29\%$

**Table 1.** Comparison of different sized cavities when needle is completely inserted inside the cavity

Cavity	Diameter (mm)	Height (mm)	Distance from centre of cavity to needle tip (mm)
1	50	50	10.0
2	63	63	16.5
3	72	72	21.0

height of a cavity increases (for a constant  $N$ ) the total change in magnetic flux density decreases. Figure 14 compares the experimental results to numerical results. Even though the experimental results increase with the size of cavity they do not fluctuate so much compared to the numerical results.

## 6 Conclusion

The application of magnetic principles in medicine has paved the way for safe, low-cost, non-invasive/minimally invasive, healthcare for patients worldwide. Superparamagnetic nanoparticles or magnetic fluid is one of the most promising advancements in the application of magnetism in biomedicine. The main feature of magnetic fluid is that it can be controlled by an external magnetic field which opens up limitless opportunities in applications such as biomolecular tagging, targeted drug delivery, MRI and hyperthermia. Magnetic fluid hyperthermia has the potential to be an effective, non-invasive cancer therapy with negligible side

effects. Magnetic fluid is injected into the affected area and an external ac magnetic field is added to exploit the self heating properties of the particles.

One of the main problems associated with magnetic fluid hyperthermia is that the magnetic fluid spreads inside tissue once injected, reducing its content density. Specific heat capacity is directly proportional to magnetic fluid content density. Inaccurate estimation of magnetic fluid content density has two major effects; i) if a low dosage is given the overall effect is thermal under-dosage in the target region which often leads to recurrent tumor growth ii) if heat given to a target region exceeds the therapeutic limit it may damage healthy cells. Hence, it can be stated that the quality of magnetic fluid hyperthermia treatment is proportional to the accuracy of estimating magnetic fluid content density inside the body. Hyperthermia therapy is most effectively performed on primary tumors. The diameter of primary tumors is typically less than 20 mm, assuming a spherical shape. Tumor sizes in stages 3 and 4 of cancer are more than 50 mm in diameter further complicating matters in retention of magnetic fluid. A novel needle-type GMR sensor was fabricated and utilized to estimate the magnetic fluid weight densities in large cavities. Theoretical analysis presenting the basis for estimating magnetic fluid weight density was presented.

Experiments were performed with agar cavities simulating cancerous tumors at various stages. The different size agar cavities were injected with magnetic fluid to simulate fluid filled tumors in cancer. The needle-type GMR sensor was then used to measure the change in the magnetic flux density. Since the cylindrical agar cavities representing tumors in the 1/2<sup>nd</sup> stage cancer were 18 mm the 20 mm needle was easily inserted into the centre to measure magnetic flux density inside the cavity. However, cavities which represent 3/4<sup>th</sup> stage tumors were 63 mm so the needle could not be inserted into the centre. Hence, a new summing method was developed to estimate magnetic fluid weight density by differential magnetic flux density. The sensing area at the tip and the bridge circuit of the design was then exploited and the change in magnetic flux density was estimated at a range of points and then summed to get the total change for a range of magnetic fluid weight densities. The results show that the change in magnetic flux density is proportional to the magnetic fluid weight density and the results fall between the theoretical lines for  $N = 0$  and 0.33 based on ellipsoidal cavities. Furthermore, it has good agreement with experimental results for small cavities of same demagnetizing factor and numerical results that simulated the actual experimental condition. Further experiments were done to measure the magnetic fluid weight density in different sized cavities for constant  $N$ . Currently hyperthermia therapy for large tumors is performed mainly to kill part of the tumor since it is difficult to accurately measure the magnetic fluid weight density inside the tumor. This makes it difficult to provide accurate heat to kill tumors and not affect healthy cells. Usually further chemotherapy and/or radiotherapy is performed in lower doses after hyperthermia therapy to completely kill the tumor. By precise estimation of magnetic fluid weight density by inside large tumors hyperthermia therapy has a good potential to be an effective treatment.

The fabricated needle-type GMR sensor has a good possibility to be used for such purpose in the future. Some positive aspects of using the method proposed

can be taken into account when considering actual clinical procedure. The needle sensor can be inserted into the body in a minimally low-invasive way. The needle-type GMR sensor has a good potential to be used in other medical applications such as targeted drug delivery where the needle-sensor can be used to confirm if the magnetic particles and drugs are present at a given site by detection as well as estimation of the content density for supplying heat to initiate a chemical reaction. Due considerations should also be given to improve some aspects of the proposed method for successful implementation in clinical applications. While the needle currently used is thin enough to be minimally invasive, it is fragile and is thus uneasy for inserting inside the human body. A needle must be designed and fabricated that would be safe to be used inside the human body. A design in the form of an acupuncture needle has the possibility of being minimally invasive as well as safe to be used inside the body. Currently it is assumed that tumors are spherical in shape. However, in reality they could be of any shape. This gives rise to the situation where the orientation of the cavity should be considered. Hence, more experiments are needed to be performed with different shapes and orientations of cavities with regards to the actual situation.

## Acknowledgement

This research was supported in part by the Foundation for Japan Science and Technology Agency, 07-029.

## References

- [1] Pankhurst, Q.A., Connolly, J., Jones, S.K., Dobson, J.: Applications of magnetic nanoparticles in biomedicine. *Journal of Physics D: Applied Physics* 36, R167–R181 (2003)
- [2] Babincova, M., Leszczynska, D., Sourivong, P., Babinec, P.: Blood-specific whole-body electromagnetic hyperthermia. *Medical Hypotheses* 55(6), 459–460 (2000)
- [3] Berry, C.C., Curtis, A.S.G.: Functionalisation of magnetic nanoparticles for applications in biomedicine. *Journal of Physics D: Applied Physics* 36, R198–R206 (2003)
- [4] Gupta, A.K., Gupta, M.: Synthesis and surface engineering of iron oxide nanoparticles for biomedical applications. *Biomaterials* 26, 3995–4021 (2005)
- [5] Jordan, A., Scholz, R., Maier-Hauff, K., Johannsen, M., Wust, P., Nadobny, J., Schirra, H., Schmidt, H., Deger, S., Loening, S., Lanksch, W., Felix, R.: Presentation of a new magnetic field therapy system for the treatment of human solid tumors with magnetic fluid hyperthermia. *Journal of Magnetism and Magnetic Materials* 225, 118–126 (2001)
- [6] Jordan, A., Scholz, R., Wust, P., Fähling, H., Felix, R.: Magnetic fluid hyperthermia (MFH): Cancer treatment with AC magnetic field induced excitation of biocompatible superparamagnetic nanoparticles. *Journal of Magnetism and Magnetic Materials* 201, 413–419 (1999)
- [7] Hilger, I., Hergt, R., Kaiser, W.A.: Towards breast cancer treatment by magnetic heating. *Journal of Magnetism and Magnetic Materials*, 314–319 (2005)

- [8] Bae, S., Lee, S.W.: Applications of NiFe<sub>2</sub>O<sub>4</sub> nanoparticles for a hyperthermia agent in biomedicine. *Applied Physics Letters* 89, 252503 (2006)
- [9] Mukhopadhyay, S.C., Chomsuwan, K., Gooneratne, C.P., Yamada, S.: A Novel Needle-Type GMR Sensor for Biomedical Applications. *IEEE Sensors Journal* 31, 401–408 (2007)
- [10] Yamada, S., Chomsuwan, K., Mukhopadhyay, S.C., Iwahara, M., Kakikawa, M., Nagano, I.: Detection of Magnetic Fluid Volume Density with a GMR Sensor. *Journal of the Magnetics Society of Japan* 31, 44–47 (2007)
- [11] Gooneratne, C., Chomsuwan, K., Łęka, A., Kakikawa, M., Iwahara, M., Yamada, S.: Estimation of Density of Low-Concentration Magnetic Fluid by a Needle-Type GMR Sensor for Medical Applications. *Journal of the Magnetics Society of Japan* 31, 191–194 (2008)
- [12] Sasada, I., Nakashima, Y.: A planar coil system consisting of three coil pairs for producing uniform magnetic field. *Journal of Applied Physics* 99(8), 08D904–08D904-3 (2006)
- [13] Gooneratne, C.P., Iwahara, M., Kakikawa, M., Yamada, S., Kurnicki, A., Mukhopadhyay, S.C.: Magnetic fluid weight density estimation in large cavities by a needle-type GMR sensor. In: *Proceedings of the 3rd International Conference on Sensing Technology 2008*, pp. 642–647. IEEE, Los Alamitos (2008)
- [14] Gooneratne, C., Łęka, A., Iwahara, M., Kakikawa, M., Yamada, S.: Estimation of Low-Concentration Magnetic Fluid Weight Density and Detection inside an Artificial Medium Using a Novel GMR Sensor. *Sensors and Transducers Journal* 90 (Special issue), 27–38 (2008)